Clinical, Cosmetic and Investigational Dermatology

Dovepress

open access to scientific and medical research

Open Access Full Text Article

ORIGINAL RESEARCH

Proteomic Analysis of Two Different Methods to Induce Skin Melanin Deposition Models in Guinea Pigs

Fei Song[1,2,*], Yan Wang[1,*], Xiao-ge Wei[1,2], Nan Yang[1], Wenjing Sun[1], Kaiying Li[1], Huisheng Ma[1,2], Jing Mu[1]

[1]College of Traditional Chinese Medicine, Ningxia Medical University, Yinchuan, Ningxia, People's Republic of China; [2]Key Laboratory of Modernization of Minority Medicine, Ministry of Education, Ningxia Medical University, Yinchuan, Ningxia, People's Republic of China

*These authors contributed equally to this work

Correspondence: Jing Mu; Huisheng Ma, Email mujing930@163.com; madoctor@163.com

Objective: In this study, we analyzed the differential expression and key signaling pathways of proteins in the skin of guinea pigs with melanin deposition caused by two different modeling methods by utilizing proteomics techniques.

Methods: Guinea pig skin melanin deposition models were: (1) induced by ultraviolet (UV) irradiation alone (U group), (2) induced by UV combined with progesterone injection (P group), and guinea pigs treated without any treatment were used as blank group (B group). H&E staining and Masson staining were used to observe the extent of skin damage and melanin deposition in guinea pigs. The differentially expressed proteins (DEPs) in the skin tissues of melanin-deposited guinea pigs were screened by proteomic techniques, the functions of DEPs were analyzed, and a protein-protein interaction network (PPI) was constructed.

Results: There was a significant difference in grayscale between the U and P groups of guinea pig skin before and after modeling ($P < 0.01$). H&E and Masson staining showed that the U and P groups both exhibited incomplete keratinization of the stratum corneum, increased proliferation of epidermal cells with large nuclei and disordered arrangement, neovascularization of the dermis, and increased the number of melanin particles in the epidermis of the U and P groups of guinea pigs compared with the B group. Proteomics analysis showed that there were 171 DEPs between the U and P groups. These DEPs focused on biological processes such as fibrillar collagen trimer, extracellular matrix containing collagen proteins, metalloproteinase activity, and peroxidase activity.

Conclusion: The melanin pigmentation model induced solely by UV radiation negatively regulates biological processes such as extracellular matrix and collagen synthesis, while inducing significant skin photoaging. The combination of progesterone injections and UV radiation-induced melanin pigmentation model can cause abnormal protein expression in fatty acid and phospholipid metabolism, possibly being closer to the environment of melasma formation.

Keywords: melasma, skin melanin, melanin deposition, ultraviolet, progesterone

Introduction

The formation of skin pigmentation and patches is a typical symptom of dermatological pigment metabolism disorders,[1] and pigmentation on the face and other exposed areas can directly affect patients' appearance and mental health. Under the stimulation of ultraviolet exposure, skin damage, pregnancy, and other factors, there is an abnormal increase in melanin secretion in the skin, leading to the accumulation of melanin in large amounts on the skin's surface, resulting in skin pigmentation.[2]

In recent years, Western and Chinese researchers have been studying the theoretical mechanisms of new drug development, and traditional Chinese medicine therapies for skin pigmentation disorders, and animal studies related to this play a crucial role. Among animal models, Chinese scholars often use KM mice, guinea pigs, etc.[3] while foreign scholars generally use C57BL/6 mice, HRM-2 hairless mice, and other animal strains.[4] Studies have shown[5,6] that animals with albinism, including KM mice, ICR mice, SD rats, and albino guinea pigs, have impaired melanin biosynthesis or abnormal melanin metabolism, and are therefore unsuitable as experimental animal models for studying

Received: 8 May 2023
Accepted: 10 August 2023
Published: 29 August 2023

skin pigmentation dysfunction. According to reports,[7,8] human epidermal thickness is 70–120 μm, while the epidermal thickness of mice is less than 25 μm and that of guinea pigs is 96 μm. Human dermal thickness is 1000–2000 μm, while that of guinea pigs is 1150–1140 μm. The thickness of mouse skin is much lower than that of humans, while the thickness of guinea pig skin is closer to that of humans. Therefore, the brown guinea pig is prioritized for experimental research on skin pigment metabolism disorders.[9]

Based on literature statistics,[3] there are various methods to establish guinea pig models of skin melanin deposition, with simple ultraviolet irradiation and ultraviolet irradiation combined with progesterone injection accounting for 43.27% and 28.85% of the model methods, respectively. From the perspective of changes in skin color, tissue pathology, and biochemical indicators, these two methods of inducing skin melanin deposition are considered relatively mature and stable. Currently, comparative experimental studies on these two model methods are rare.

In addition, proteomic techniques have been widely used to study the pathogenesis of various diseases. Schafer et al, through proteomics, revealed new regulatory proteins and pathways associated with tumorigenicity and progression of cutaneous squamous cell carcinoma caused by cutaneous human papillomavirus (HPV) infection combined with chronic ultraviolet (UV) exposure.[10] In the study of Hedrich et al, proteomics was used to characterize the role of PRAME (preferentially expressed antigen in melanoma) to reveal that PRAME is the true target of endogenous Gas6/Axl activation in tumors by promoting epithelial-mesenchymal transformation and invasion of cancer cells in hepatocellular carcinoma.[11] In addition, it is worth mentioning that it is well known that proteins are an important component of cellular structure and also an important embodiment of cellular and biological functions. Therefore, it is of great significance to explore the molecular mechanism of skin melanin-related diseases at the protein level. Therefore, this study aims to explore the differences in the molecular mechanisms of skin melanin deposition induced by these two methods from the perspective of proteomics, so as to provide references for the research of pigmentation related diseases and the establishment of relevant experimental animal models.

Materials and Methods

Experimental Animals

The experimental animals were provided by Ningxia Medical University (license number: SYXK (Ning) 2020-0001) and housed at the Animal Experimental Center, Shuangyi Campus, Ningxia Medical University. The animal experiments were reviewed and approved by the Animal Ethics Committee of Ningxia Medical University (IACUC-NYLAC-2021-070). Standard regulations were followed for the housing of the experimental guinea pigs, which were provided with standard water, standard guinea pig feed, and appropriate amounts of fresh cabbage. The room was maintained at a temperature of around 26 °C and a humidity of 50–60%. This study strictly followed the ARRIVE Guidelines 2.0 published in animal experiments for conducting animal experiments. And we have always adhered to the Animal welfare principles in the NIH Guide for the Care and Use of Laboratory Animals.

Experimental Groups

Fifteen healthy female guinea pigs of normal grade (2 months old, 400 ± 50 g) were randomly divided into a blank group (B group), an ultraviolet radiation group (U group), and a combination of progesterone injection and ultraviolet radiation group (P group), with 5 animals in each group.

Model Construction

Production of an Experimental UV Light Box

Nine 313 nm UVB lamps were selected and arranged in a well-alternating pattern to produce a UV light box that could uniformly irradiate 12 guinea pigs. The irradiation height was set at 15 cm. When the UV light box was turned on, the UV radiation intensity at the bottom of the box was measured by a radiometer and found to be 0.60 mW/cm^2.

Construction of U Group Model

After one week of adaptive feeding for guinea pigs, hair removal cream was applied every other day to remove the hair on the back of the guinea pig, within an area of approximately 4×4 cm. The guinea pig was then placed in the UV light

box, and each irradiation time was set to 25 mins with a single radiation dose of 900 mJ/cm^2. Within 14 days, a total of 7 times of UVB irradiation was given, with a total cumulative dose of 6300 mJ/cm^2.

Construction of P Group Model

After one week of adaptive feeding for guinea pigs, the P group guinea pigs were treated with the same frequency and irradiation dose as that of the U group. In addition, every other day, 20 mg/kg of progesterone was injected into the posterior muscle group of one of the hind legs of the guinea pig. The injections were alternated between both hind legs, and a total of 7 injections were given.

Analysis of Guinea Pig Skin Images Using ImageJ Software

One day prior to preparing the pigmentation model and on the 14th day after modeling, hair was removed from the back of the guinea pig using depilatory cream, leaving an area of approximately 4×4 cm. The area was kept clean, and under natural light, photographs of the skin on the back of each guinea pig were taken. ImageJ 2.9 software was used to process the images and compare the grayscale values of the skin before and after modeling.

Subsequently, the guinea pigs were euthanized by intraperitoneal injection of 2% sodium pentobarbital. Along the boundaries of the irradiated area on the guinea pig's skin, quickly peel off the skin from the back and place it on an ice box. Rinse the skin thoroughly with physiological saline to remove any blood clots and subcutaneous fat. Cut the cleaned skin into small pieces and measure. Immediately place one piece into a cryovial and freeze it rapidly in a liquid nitrogen tank for subsequent proteomic analysis. The other portion of skin tissue was used for tissue sectioning.

Hematoxylin and Eosin (H&E) and Masson Staining

Skin tissue was cut into approximately 0.5 cm × 0.5 cm pieces according to the experimental requirements. The tissue was quickly washed with pre-cooled physiological saline to remove any blood, placed in a labeled embedding box, fixed in 4% paraformaldehyde solution for 24 hours, and subjected to H&E and Masson staining. Tissue pathological observations were made using an optical microscope.

On-Machine Protein Mass Spectrometry

Mass Spectrometry Chromatography Conditions

The mass spectrometry adopts a data-dependent acquisition mode, with a full scan range of 350–1550 m/z, a primary mass spectrometry resolution of 120,000 (200 m/z), AGC of 3×10^6, and a maximum injection time of 80 ms. The top 40 ions with the highest intensity from the full scan are selected for high-energy collision-induced dissociation (HCD) fragmentation and secondary mass spectrometry detection. The secondary mass spectrometry resolution is set to 15,000 (200 m/z), AGC is 5×10^4, and the maximum injection time is 45 ms. The peptide fragmentation collision energy is set to 27%, generating raw mass spectrometry detection data (.raw).

DIA Sample On-Machine

The mass spectrometry adopts a data-independent acquisition (DIA) mode, with a full scan range of 350–1500 m/z, a primary mass spectrometry resolution of 60,000, a maximum capacity of C-trap of 3×10^6, and a maximum injection time of C-trap of 50 ms. The peptide fragmentation collision energy is set to 25.5%, 27%, and 30%.

Database Search

In the UniProt database, the guinea pig proteomics data were selected. Spectronaunt's built-in Pulsar was used for data retrieval, and a spectral library was established using DDA data and DIA data.

Analysis and Screening of Differentially Expressed Proteins (DEPs)

Principal component analysis (PCA) was performed on three groups of skin samples to preliminarily understand the overall differences between the groups and the variability within each group. Upregulated proteins were selected when the fold change (FC) was greater than or equal to 1.5 and the p-value was less than or equal to 0.05. Downregulated proteins were selected when the FC was less than or equal to 1/1.5 and the p-value was less than or equal to 0.05.

Protein-Protein Interaction Network (PPI)

DEPs were input into the STRING database (http://string-db.org/) to find interactions between proteins using a minimum interaction score threshold of 0.4 (medium confidence).[12] The TSV format file of PPI was downloaded and imported into Cytoscape software to construct the PPI network. Clustering and enrichment analysis of proteins with network interactions was performed using the ClueGO and Cluepeadia plugins built into Cytoscape.[13]

Statistical Analysis

The means and standard deviations of different treatments were compared and visualized using GraphPad Prism 9.5 software. One-way ANOVA was performed and *t*-tests were used for significance analysis, where $p < 0.05$ indicated a statistically significant difference.

Results

Comparison of Skin Color in Guinea Pigs

After 14 days of intervention, the skin on the exposed areas of the U and P groups of guinea pigs became significantly darker, with an increase in black spots and merging. There was no apparent difference in skin color between the U and P groups as observed by the naked eye. The grayscale values of skin photos of the two groups of guinea pigs showed no statistical difference ($P > 0.05$) before and after modeling. However, there was a significant difference between the U and P groups before and after modeling ($P < 0.01$) (Figure 1A–E).

Histological Analysis of Guinea Pig Skin with H&E and Masson Staining

To gain a more detailed understanding of the morphological changes and melanin deposition of the guinea pig skin, we performed H&E and Masson staining followed by optical microscopy observation (Figure 2A and B). In the B group, the stratum corneum was intact, with minimal melanin particles visible in the basal layer. The fibrous tissue in the dermal layer was well-ordered, and there was no noticeable infiltration of inflammatory cells. The hair follicles and sebaceous gland structures were intact. In the U group, the stratum corneum was thinner, and a large number of melanin particles were visible in the basal and spinous layers. The fibrous tissue in the dermal layer was disordered, and the outlines of the hair follicles and sebaceous glands were enlarged. In the P group, the stratum corneum was also thinner, with a large number of melanin particles visible in the basal and spinous layers. The fibrous tissue in the dermal layer was moderately disordered, and the outlines of the hair follicles and sebaceous glands were enlarged.

DEPs Identification and Annotation

After quality control inspection, two samples from group B were classified as Grade C, which were excluded to ensure the reliability of the results. A total of 4816 proteins were identified from the remaining 13 guinea pig skin samples. Based on different treatment methods, the samples were divided into three groups for principal component analysis (PCA) (Figure 3A), which revealed a significant difference in overall diversity between the B, U, and P groups. In contrast, samples within each group showed high similarity. The identified proteins were functionally annotated using the GO, KEGG, and COG databases to understand their functional characteristics. Among the annotated protein genes, GO was able to annotate 4470, KEGG was able to annotate 2384, and COG was able to annotate 2119 proteins (Figure 3B).

GO and Kyoto Encyclopedia of Genes and Genomes (KEGG) Enrichment Analysis

The GO enrichment analysis (Figure 4A) was carried out on annotated guinea pig skin proteins. The DEPs for cellular component were mainly located in components include cells, cell parts, and organelles. In molecular function, DEPs were mainly associated with binding, catalytic activity, and molecular function regulation. In terms of biological process, DEPs were mainly enriched in cellular processes, single-organism processes, and bioregulation.

The annotation results of guinea pig skin proteins in the KEGG (Figure 4B) indicated that DEPs were mainly involved in cellular processes including endocytosis, focal adhesion, and phagosomes. They also participated in the regulation of signaling pathways including the Pl3K-Akt pathway, MAPK pathway, and calcium signaling pathway. In terms of genetic information processing, these proteins mainly affected protein processing in the endoplasmic reticulum,

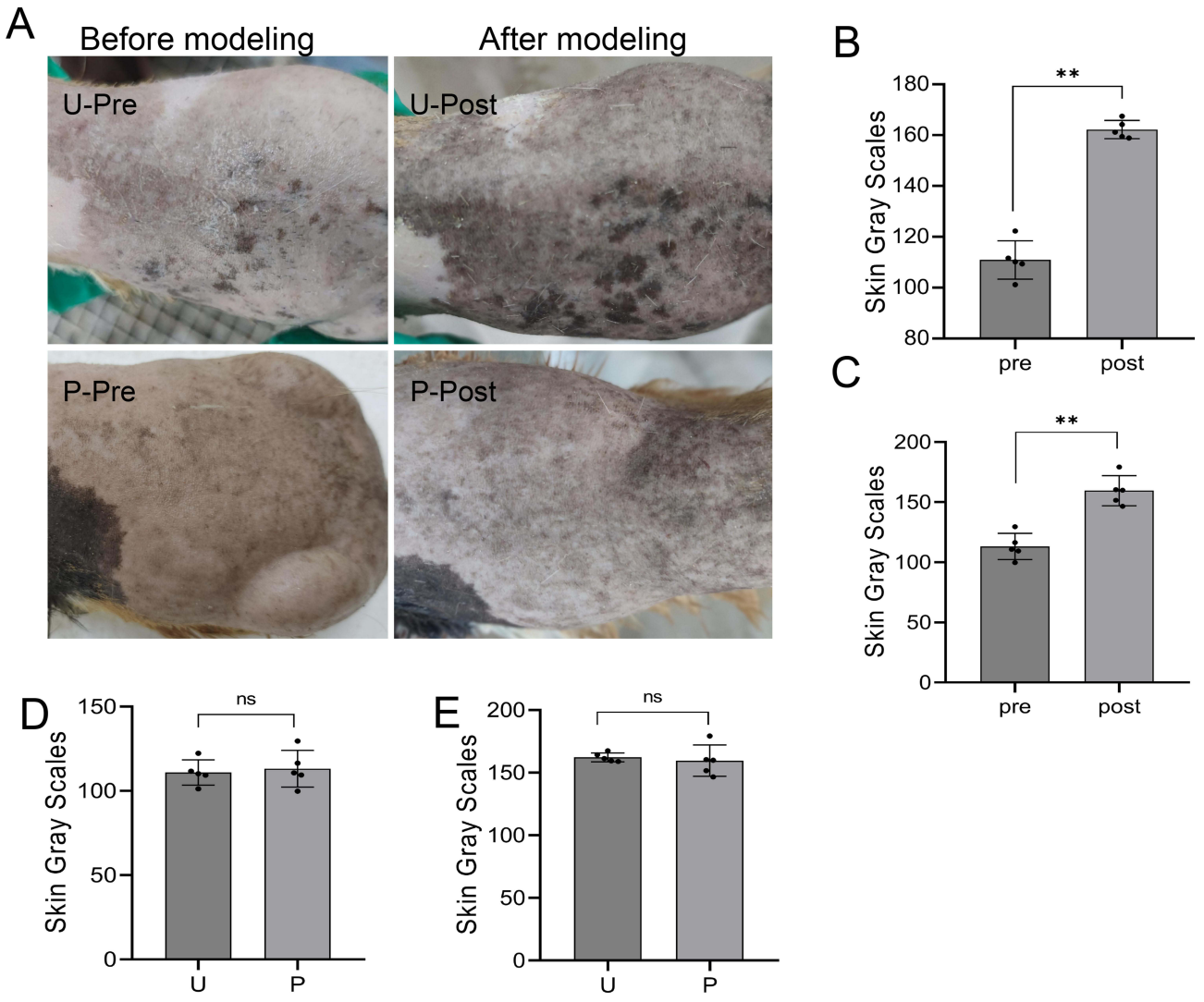

Figure 1 Color comparison of the skin of the two groups before and after the molding. (**A**) Representative pictures of skin color changes on the back of Guinea pigs in groups U and P before and after modeling. (**B**) Gray scale statistical analysis results of back skin of Guinea pigs in group U before and after modeling. (**C**) gray scale statistical analysis results of back skin of Guinea pigs in group P before and after modeling. (**D**) Gray scale statistical analysis results of back skin of Guinea pigs in groups U and P before modeling. (**E**) statistical analysis results of gray scale of back skin of Guinea pigs in groups U and P after modeling. Note: ** represents $P < 0.01$, ns represents $P > 0.05$. U group: an ultraviolet radiation, P group: a combination of progesterone injection and ultraviolet radiation.

spliceosome, and nucleotide transport. In relation to human diseases, the proteins were mainly associated with cancer, bacterial and viral infectious diseases. In the metabolic processes, they participated in oxidative phosphorylation, carbon metabolism, and purine metabolism. Their effects on the organism's systems included insulin signaling pathways, oxytocin signaling pathways, and adrenergic signaling in cardiac myocytes.

Identification of DEPs Between the Three Groups

As shown in Figure 5A, a total of 191 DEPs were identified between the U and B groups, with 147 upregulated DEPs and 44 downregulated DEPs. And a total of 244 DEPs were identified between the P and B groups, with 233 upregulated DEPs and 11 downregulated DEPs (Figure 5B). As shown in Figure 5C, a total of 171 DEPs were identified between the P and U groups, with 146 upregulated DEPs and 25 downregulated DEPs. Two common DEPs were found when comparing the three groups. In addition, there were 40 commonly DEPs in the B vs U and B vs P group comparisons, 13 in the B vs U and U vs P group comparisons, and 45 in the B vs P and U vs P group comparisons (Figure 5D).

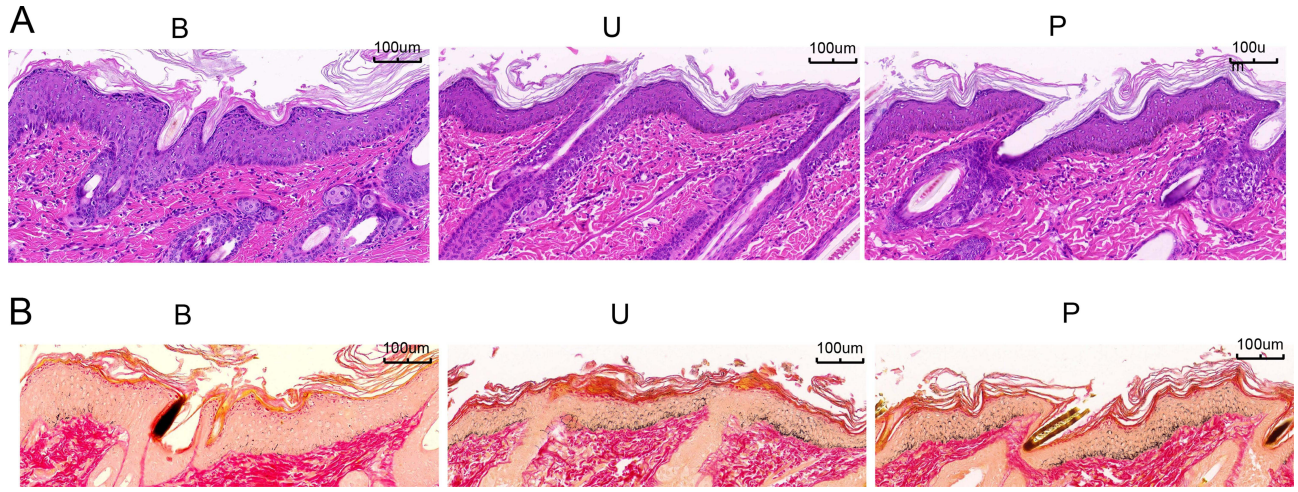

Figure 2 H&E and Masson staining (× 100). (**A**) H&E staining was used to detect the pathological changes of Guinea pig skin. (**B**) Masson staining was used to detect melanin deposition in Guinea pig skin tissue. B group: blank group, U group: an ultraviolet radiation, P group: a combination of progesterone injection and ultraviolet radiation.

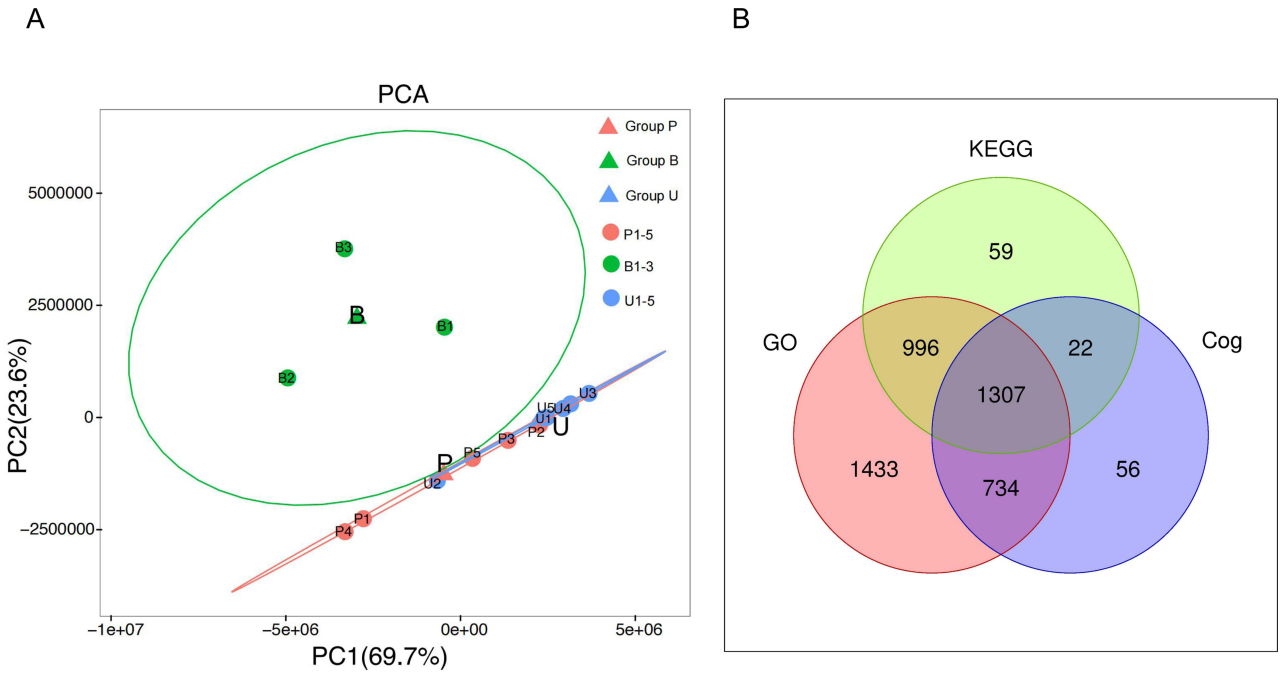

Figure 3 Principal component analysis (PCA) and the number of proteins identified in the GO, KEGG, and COG databases. (**A**) Principal component analysis of skin samples from three groups of Guinea pigs. (**B**) Venn diagram of proteins screened by GO, KEGG and COG databases.

Functional Enrichment Analysis of DEPs Between the Three Groups

The functional enrichment of DEPs between the three groups was further analyzed by GO and KEGG, respectively. For the B and U groups, GO analysis showed that the 191 DEPs were mainly enriched in protein inhibition, phenylalanine 4-monooxygenase activity, and 4-α-hydroxytetrahydrobiopterin dehydratase activity of MF, the response of cells to amino acid stimulation, extracellular matrix components, and vesicles of CC, bacterial aggregation induction, negative regulation of endothelial cell apoptosis, and positive regulation of peptide hormone secretion of BP (Figure 6A–C). From the KEGG signal pathway analysis (Figure 6D), it was found that the DEPs were mainly enriched in the arachidonic acid metabolism, platelet activation α-linolenic acid metabolism, and Fcε-RI signal pathway.

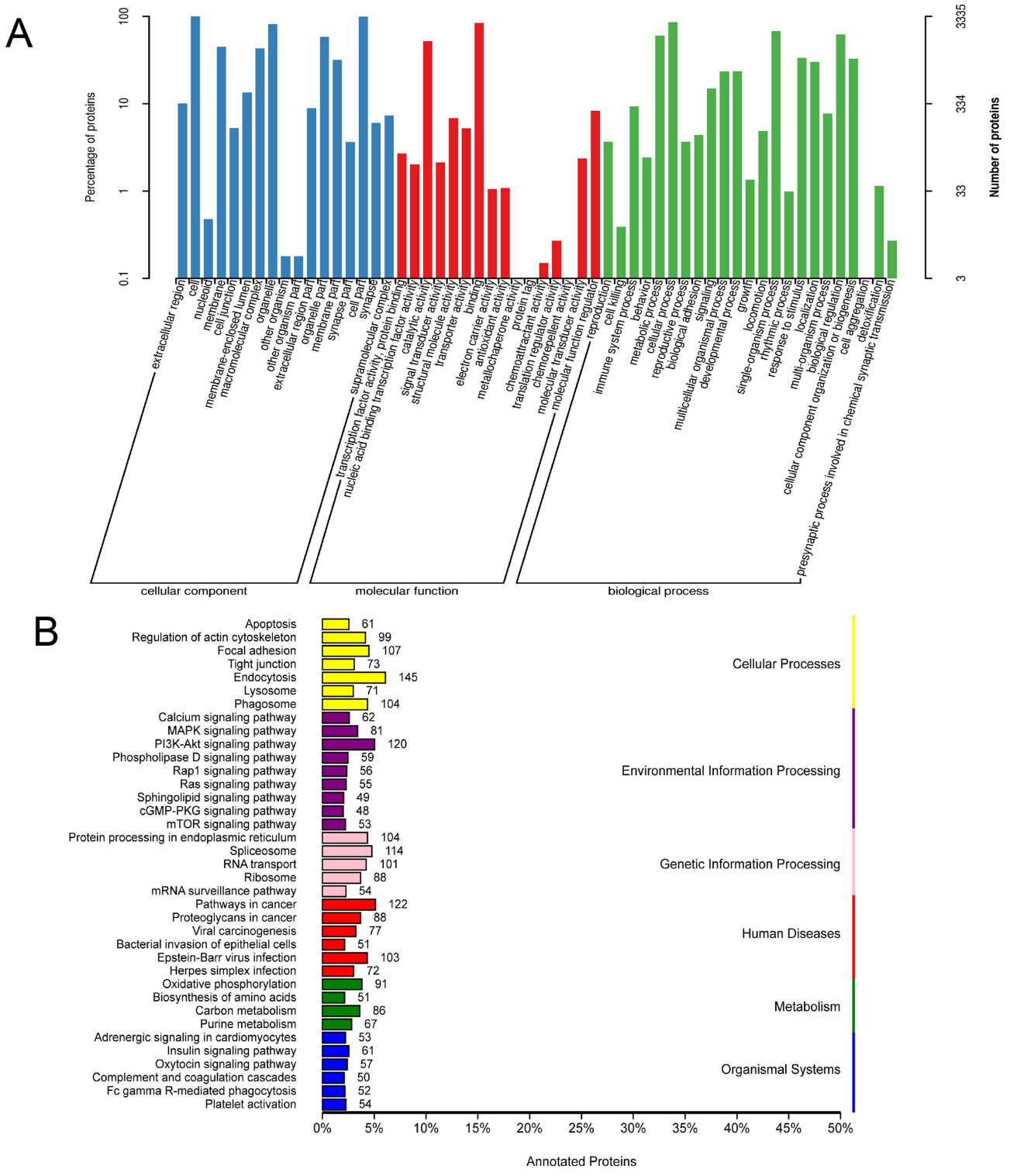

Figure 4 GO and KEGG classification annotation diagram. (**A**) GO enrichment analysis results, including cell components, molecular functions and biological processes. (**B**) KEGG enrichment analysis results.

In the B and P groups, the 244 DEPs were closely related to MF including DNA double-strand methylation, methyl-CpG binding and ATP enzyme activity, CC including vacuole proton transport V-type ATPase complex, CIA complex and MMXD complex, and BP including respiratory gas exchange, mannose metabolism process and social behavior

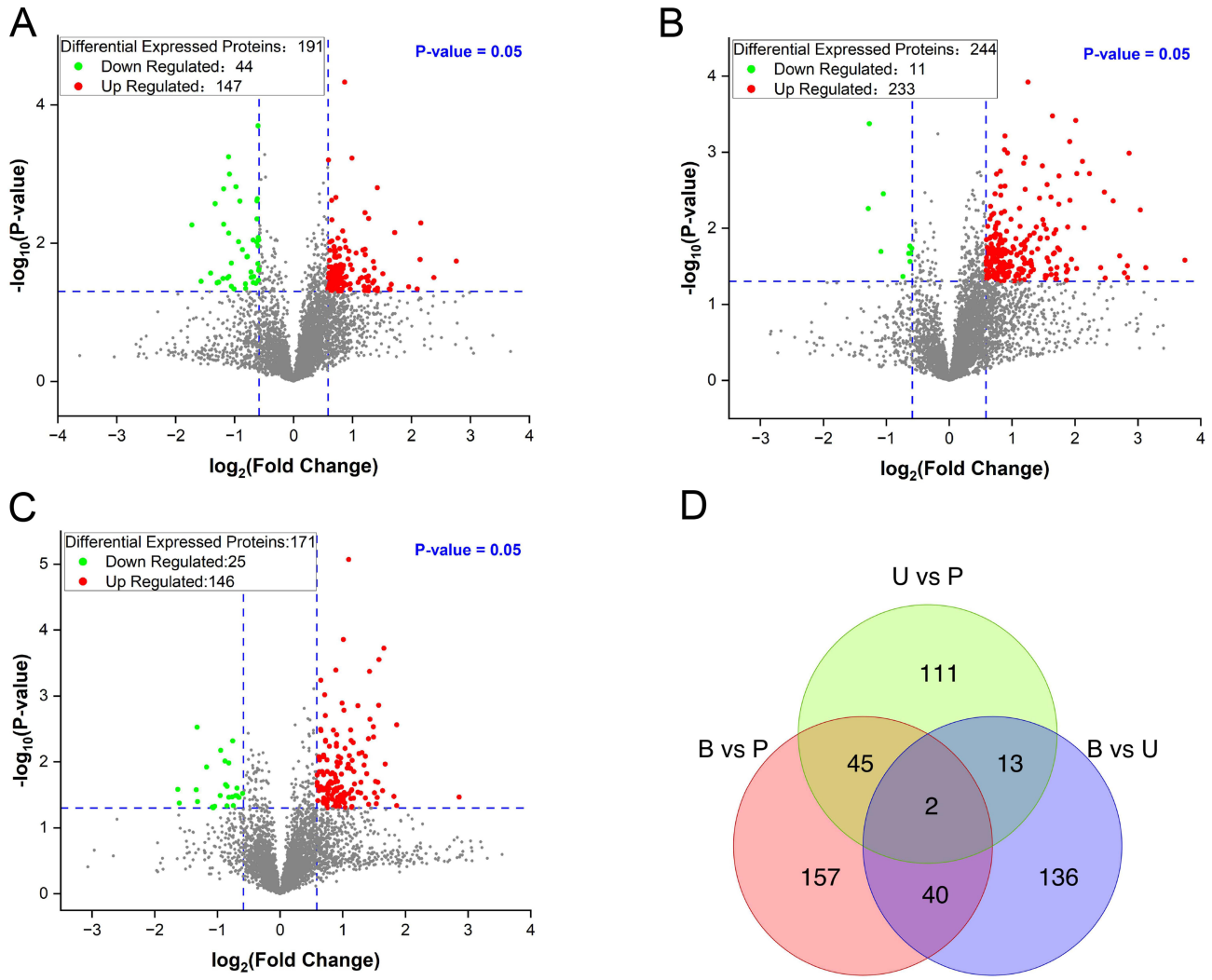

Figure 5 The volcano plot and Wayne plot of the differential expressed proteins (DEPs). (**A**) Volcano map of DEPs between the group U and group B. (**B**) Volcano map of DEPs between the group P and group B. (**C**) Volcano map of DEPs between the P and U groups. (**D**) Wayne plot of DEPs in each comparative group. B group: blank group, U group: an ultraviolet radiation, P group: a combination of progesterone injection and ultraviolet radiation.

(Figure 7A–C). Moreover, KEGG analysis (Figure 7D) showed that the DEPs were mainly associated with glycophospholipid metabolism, GPI-anchor biosynthesis, and nucleotide transport.

For the B and P groups, GO enrichment analysis showed that the 171 DEPs were mainly enriched in platelet-derived growth factor binding, protease binding, oxidoreductase activity, copper ion binding and metallopeptidase activity of MF, extracellular matrix structural components, cellular response to amino acid stimulus, and extracellular space of CC, collagen fiber organization, blood vascular development and skin morphogenesis of BP (Figure 8A–C). The KEGG analysis (Figure 8D) revealed that the DEPs were mainly involved in protein digestion and absorption, AGE-RAGE signaling pathway in diabetic complications, and asthma.

PPI Construction and Module Analysis

To further investigate the differences between the two guinea pig skin melanin deposition models, the functional networks of the 171 DEPs in the U and P groups were analyzed. In terms of MF, the DEPs were involved in functions including flavin adenine dinucleotide binding, copper ion binding, peroxidase activity, collagen binding, and metalloendopeptidase activity (Figure 9A). In terms of CC, the DEPs are mainly located in the extracellular matrix containing collagen, tropocollagen trimer, and basement membrane (Figure 9B). The DEPs were mainly related to BP, including

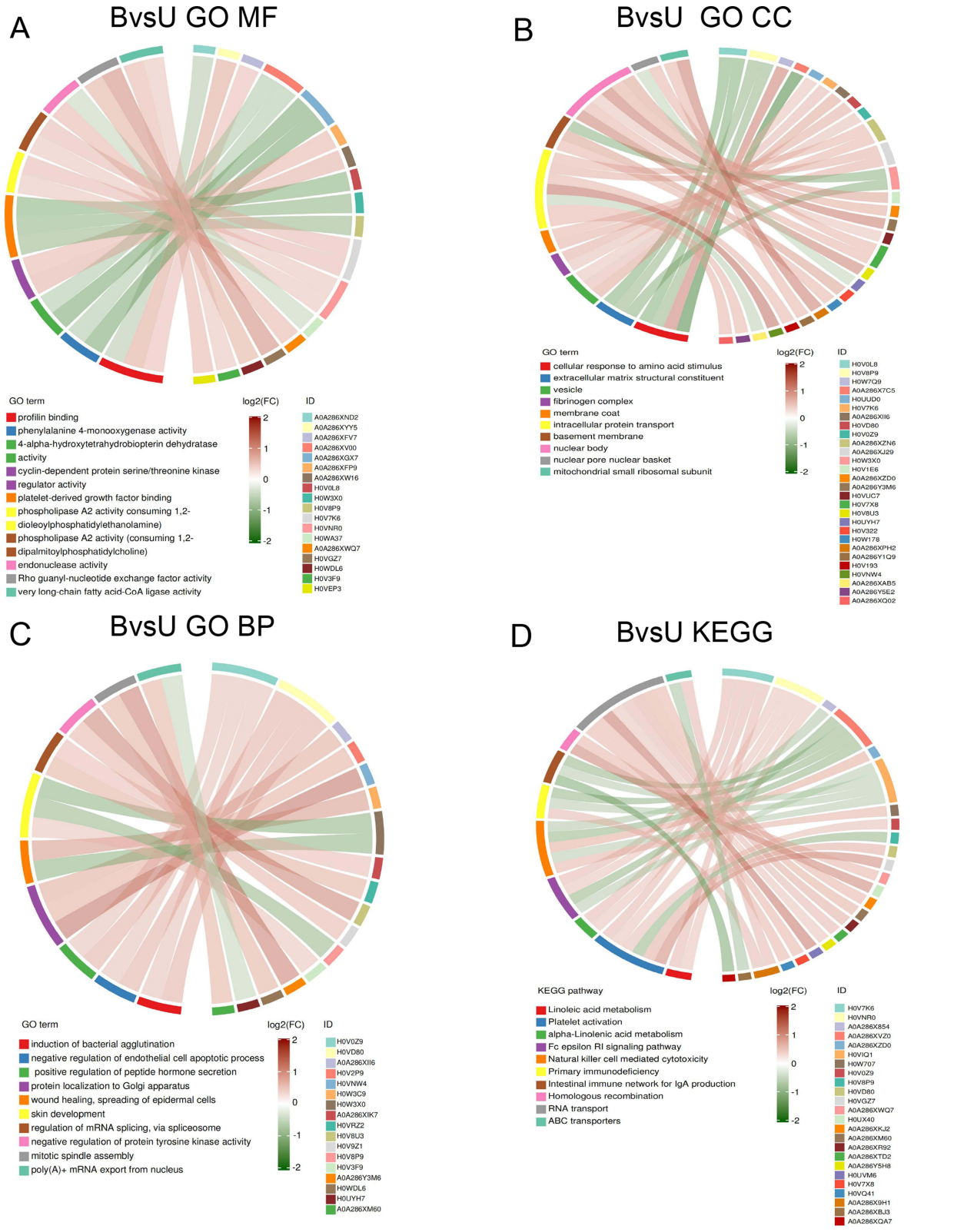

Figure 6 Enrich circos plot of the differentially expressed protein (DEPs) between the group U and group B. (**A**) Molecular functional (MF) enrichment analysis. (**B**) Cell component (CC) enrichment analysis. (**C**) Biological process (BP) enrichment analysis. (**D**) Kyoto encyclopedia of genes and genomes (KEGG) analysis of DEPs. B group: blank group, U group: an ultraviolet radiation.

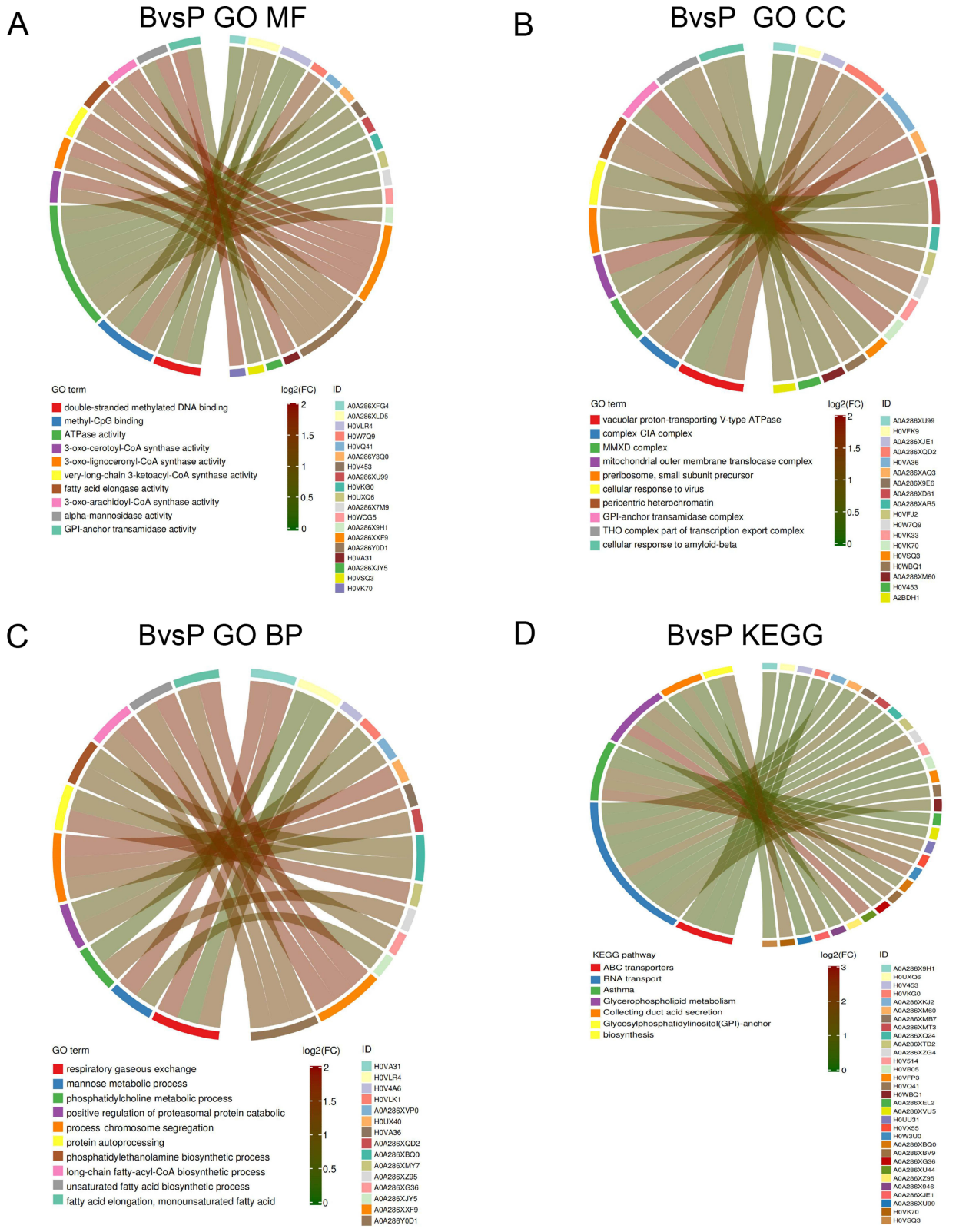

Figure 7 Enrich circos plot of the differentially expressed protein (DEPs) between the group P and group B. (**A**) Molecular functional (MF) enrichment analysis. (**B**) Cell component (CC) enrichment analysis. (**C**) Biological process (BP) enrichment analysis. (**D**) Kyoto encyclopedia of genes and genomes (KEGG) analysis of DEPs. B group: blank group, P group: a combination of progesterone injection and ultraviolet radiation.

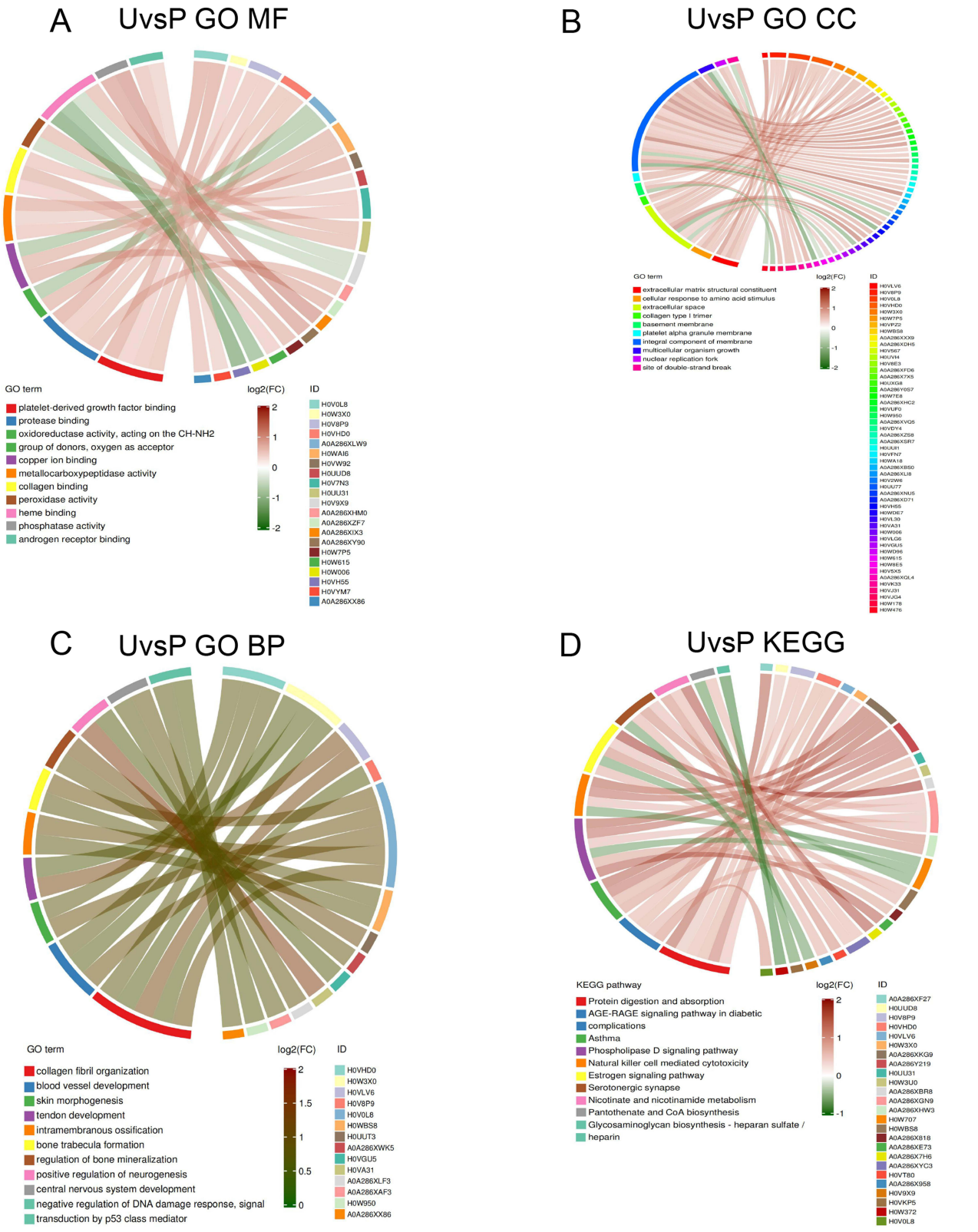

Figure 8 Enrich circos plot of the differentially expressed protein (DEPs) between the group P and group U. (**A**) Molecular functional (MF) enrichment analysis. (**B**) Cell component (CC) enrichment analysis. (**C**) Biological process (BP) enrichment analysis. (**D**) Kyoto encyclopedia of genes and genomes (KEGG) analysis of DEPs. U group: an ultraviolet radiation, P group: a combination of progesterone injection and ultraviolet radiation.

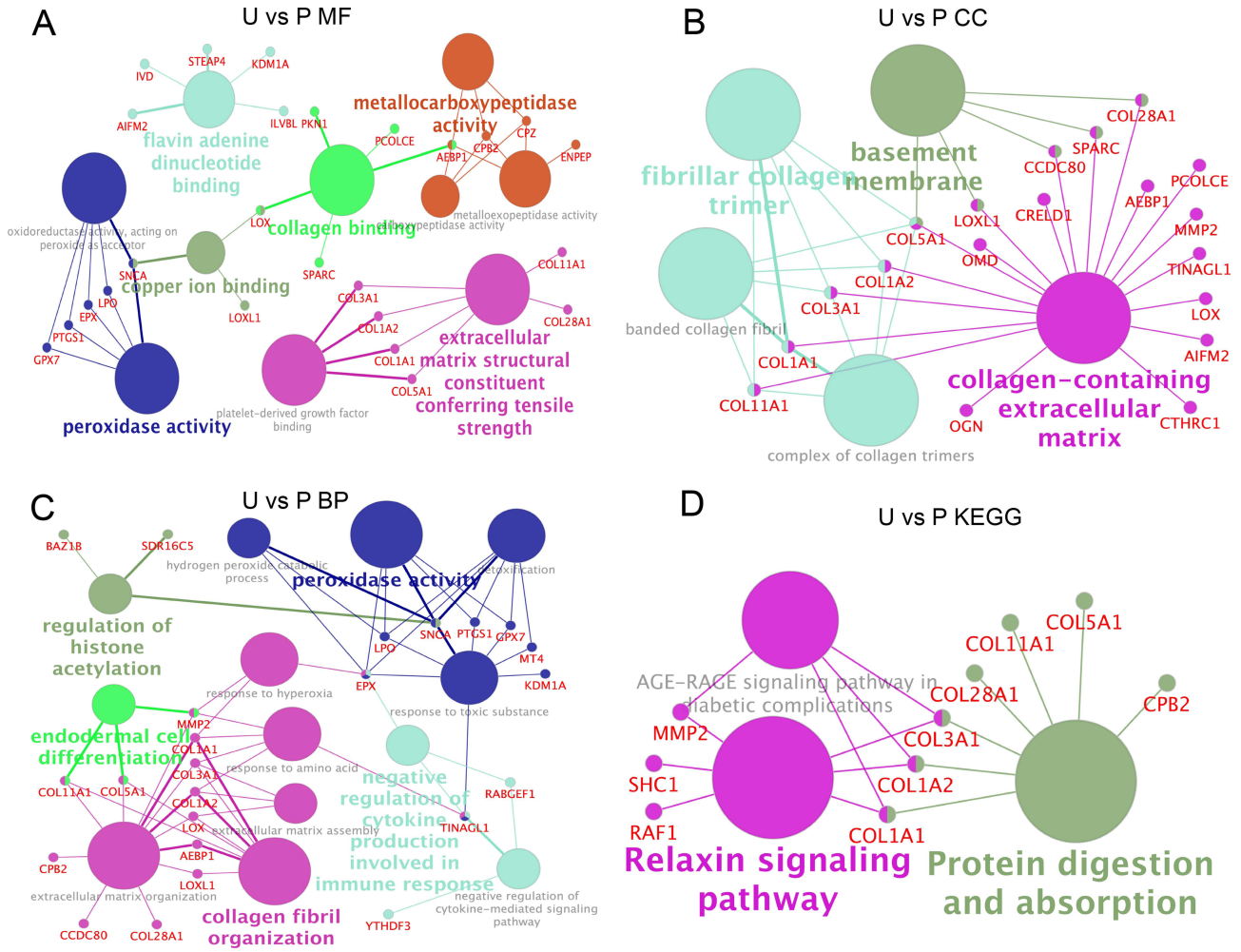

Figure 9 Functional network analysis of the differentially expressed protein (DEPs) between the group P and group U. (**A**) Network enrichment analysis of molecular functions (MF). (**B**) Network enrichment analysis of cell components (CC). (**C**) Network enrichment analysis of biological processes (BP). (**D**) Network enrichment analysis of the KEGG analysis. U group: an ultraviolet radiation, P group: a combination of progesterone injection and ultraviolet radiation.

regulation of histone acetylation, differentiation of inner cell mass cells, and collagen fiber organization, peroxidase activity (Figure 9C). The KEGG signaling pathways of DEPs mainly included the relaxin signaling pathway and protein digestion and absorption (Figure 9D).

Furthermore, we retrieved 167 relevant genes with the keyword "Melanin" from AmiGO2 (http://amigo.geneontology.org/amigo/landing), and removed duplicates. We then matched these genes with those in the STRING database for species of guinea pigs, resulting in 56 key genes. Using Cytoscape, we performed PPI analysis on the differentially expressed genes in the B vs U and B vs P groups, as well as the 56 relevant genes. We found 36 upregulated and 10 downregulated genes in the B vs U group that are associated with melanin, with the interacting proteins mainly being HTT, FECH, PAIP1, PDK3, NFATC1, ITGA9, ARL15, FKBP15, CASP6, and COL1A1. We also found 57 upregulated genes in the B vs P group associated with melanin, with the interacting proteins mainly being GAK, ACTG1, POLR2F, GNA11, HPX, Rps15, EPX, SP1, KPNA6, and MECP2 (Figure 10).

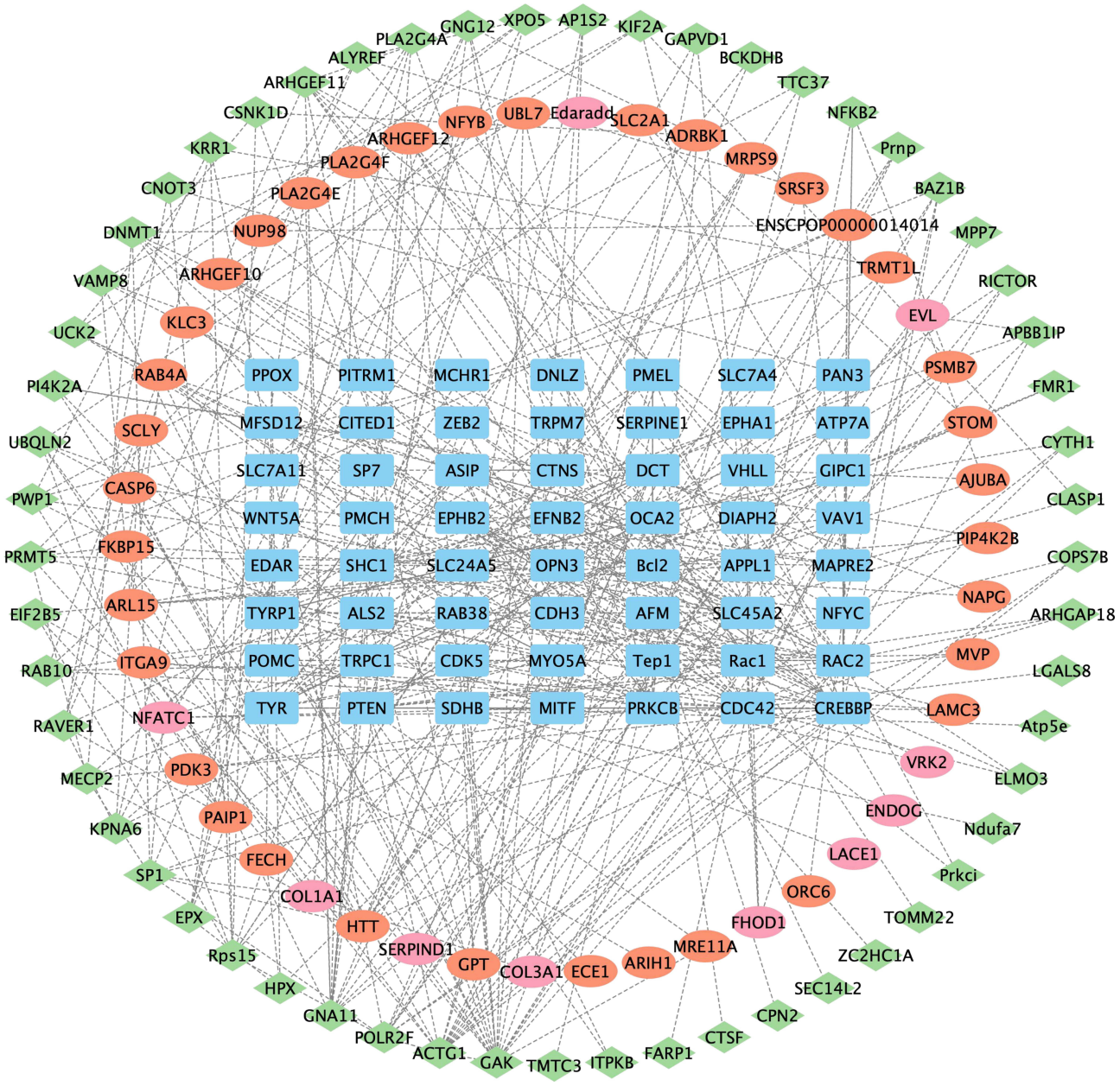

Figure 10 Differential protein and melanin-related gene PPI. The rectangles (in blue) represent key melanin genes, the ellipses (in red) represent the differentially upregulated genes in the B vs U group, the ellipses (in pink) represent the differentially downregulated genes in the B vs U group, and the diamonds (in green) represent the differentially upregulated genes in the B vs P group. The genes in each group are arranged in order of Betweenness Centrality values. B group: blank group, U group: an ultraviolet radiation, P group: a combination of progesterone injection and ultraviolet radiation.

Discussion

In this study, we found through histopathological observation and proteomic analysis that the guinea pig skin model after progesterone injection combined with ultraviolet irradiation is closer to the pathogenesis and mechanism of melanin deposition. Therefore, this model can well simulate the occurrence of human melanin deposition, so it can be further explored and even promoted in future studies.

Melanin plays a crucial role in protecting human skin from harmful UV damage.[14] However, excessive melanin can cause skin diseases including melasma, age spots, and even cancer.[15] Therefore, there is an increasing amount of research focusing on diseases related to abnormal melanin production and deposition. These researchers urgently need animal models that are safe, stable, and easy to operate, with potentially personalized requirements. In this article, we will

analyze model preparation methods, choice of evaluation indicators, and protein mechanism differences in two melanin deposition models.

Common animal experimental models for melanin deposition preparation methods include ultraviolet irradiation, progesterone injection, combined ultraviolet irradiation and progesterone injection, combined ultraviolet irradiation and topical application of estradiol, etc. However, there are currently no authoritative standards. Western scholars often use ultraviolet irradiation in modeling methods.[4] Research reports the minimum erythema dose of UVB on guinea pig skin to be 200–300 mJ/cm^2.[16] The local energy of ultraviolet radiation of 2–3 times the minimum erythema dose (ie 500–900 mJ/cm^2) is the single-dose scheme selected by most researchers. It can control the occurrence of erythema scars and form uniform pigmentation. The total UVB radiation dose selected in most literature is within the range of 2000–7500 mJ/cm^2, but the frequency of irradiation differs. Most researchers choose to irradiate once every other day.[4] Progesterone can increase melanin by increasing the number of melanocytes and the activity of key enzymes in the melanin synthesis process.[17] A study reported that there was no difference in gene expression of estrogen receptor β and progesterone receptor between skin affected by melasma and adjacent healthy skin.[18] However, the protein expression of these receptors was higher, indicating that estrogen and progesterone are involved in the pathogenesis of this disease. Meanwhile, other studies have reported weak expression of estrogen and progesterone receptors in male melasma patients.[19] There is currently no standardized indicator of the total dose of progesterone injection, and researchers often decide based on the actual situation of pigmentation in experimental animal skin. In this study, the single dose of UVB irradiation selected was 900 mJ/cm^2, irradiated once every other day, and the total irradiation dose was 6300 mJ/cm^2; the single dose of progesterone injection selected was 20 mg/(kg.day). Due to its blood concentration lasting for 48 hours in the body,[20] the injection frequency is synchronized with ultraviolet irradiation, with a once-every-other-day injection schedule, for a total of 7 injections. Ultimately, both modeling methods resulted in evident melanin pigmentation.

To judge the success of the guinea pig skin melanin deposition model, researchers mostly rely on observation of changes in skin color and histopathological analysis.[21] According to some studies,[3,22] local histopathology is the gold standard for evaluating animal models of melanin deposition and a measure of the efficacy of drug treatment for pigmentary diseases. Based on the results of this study, the U group and P group showed a significant increase in melanin particles after Masson staining compared to the B group, indicating the success of the model. However, there was no significant difference observed in pigmentation through conventional methods of observation, including visual observation of guinea pig skin color, microscopic observation of melanin particles, or computing gray values using ImageJ software. Therefore, conventional observation methods may not distinguish between these two types of models effectively. Application of proteomic techniques to observe the differential expression of related proteins may be able to provide clearer distinctions between different models of melanin deposition.

Proteomics techniques can be utilized to identify differences in gene and protein expression during the process of melanin synthesis after intervention with two modeling methods. According to literature reports,[23] more than 125 genes can regulate melanin deposition. They regulate the survival, differentiation, maturation, and production of melanocytes through specific enzymes and structural proteins. The most important positive regulatory factor in the melanin biosynthetic pathway is the MC1 receptor and its ligand, alpha-melanocyte-stimulating hormone (α-MSH); activation of MC1R stimulates the cyclic adenosine monophosphate (cAMP) response element binding protein (CREB).[24] An increase in MITF expression activates tyrosinase (TYR), tyrosinase-related protein-1 (TYRP1), and dopachrome tautomerase (DCT) through phosphorylation, thereby producing melanin.[25] In this study, we first screened for genes related to melanin using the AmiGO2 database and matched pigmented protein genes from the String database belonging to guinea pigs. We then used these genes to create a PPI network between DEPs in the B vs U and B vs P groups, and found that the DEPs in both groups were directly or indirectly related to genes associated with melanin. This suggests that the two different modeling methods may regulate the expression of different proteins to ultimately promote melanin synthesis. U Group regulates the synthesis pathway of melanin via the proteins CASP6, HTT, NFATC1, PAIP1, PDK3, FKBP15, ARL15, COL1A1, and etc., while P Group regulates the synthesis of melanin through the proteins MECP2, POLR2F, SP1, Rps15, GNA11, EPX, HPX, among others.

Proteomic analysis results show that during the process of ultraviolet-induced melanin pigmentation, compared to B group, U group guinea pig skin regulates various biological processes including skin development, epidermal cell diffusion, endothelial cell apoptosis, vascular contraction, skin healing, tyrosinase activity, and shear body. Compared to P group, not only does U group induce melanin pigmentation, but it also involves more differential proteins in the negative regulation of extracellular matrix and collagen synthesis. Studies have shown[26] that the molecular mechanism of skin photoaging is mainly caused by the reduction of extracellular matrix. Therefore, simple ultraviolet irradiation not only induces melanin pigmentation, but also accelerates the loss of skin collagen, making this model suitable not only for melanin pigmentation, but also for photoaging formation.

Comparing B and P groups, it was found that the combination of progesterone injection and ultraviolet irradiation caused more fatty acid metabolism and proteolytic metabolism. Proteomic analysis showed that the molecular mechanism activity related to the generation of extracellular matrix and collagen protein was higher in P group than in U group, indicating that after the same dose of UVB irradiation, the degree of photoaging in P group guinea pig skin was milder than that in U group. Studies have shown[27] that the main factors of chloasma formation are genetic susceptibility, exposure to sunlight, and changes in sex hormone levels. Its clinical manifestations are mainly darkening of the skin, erythema of the skin lesions during the active stage, proliferation of melanocytes under the microscope, and dendritic elongation.[28] The P group model formed a melanin deposition model under the double stimulation of excessive UVB irradiation and progesterone-induced estrogen imbalance. Therefore, the guinea pig skin model after progesterone injection combined with ultraviolet irradiation treatment may be closer to the pathogenesis and mechanism of chloasma.

Conclusion

In this study, two methods were used to induce skin melanin deposition in guinea pigs. We found that simple UV radiation treatment of guinea pig skin not only caused melanin deposition, but also promoted skin photoaging. By injecting progesterone and combined with UV radiation intervention, a method similar to the inducing factors of chloasma was used, which can also cause multiple patchy pigmented deposits on guinea pig skin. Therefore, it is inferred that this method may be applicable to the animal model research of chloasma. The results of this study provide data for the skin melanin deposition model and provide a theoretical basis for basic and clinical experimental research in relevant fields in the future. Although simple animal experiments can simulate the complex process of melanin synthesis and deposition, there may be certain limitations in molecular mechanism research. In the future, our research group will continue to conduct further verification of the molecular mechanisms that affect melanin synthesis in melanocyte culture experiments, providing more powerful biological evidence.

Data Sharing Statement

The data used to support the findings of this study are available from the corresponding author upon request.

Ethical Approval

The animal experiments were reviewed and approved by the Animal Ethics Committee of Ningxia Medical University (IACUC-NYLAC-2021-070).

Funding

This work was supported by Ningxia Natural Science Foundation Project (2023AAC03158); National Natural Science Foundation of China Regional Science Foundation (81960893); Ningxia Medical University Special Talent Start-up Project (XT2022017).

Disclosure

Fei Song and Yan Wang contributed equally to this work as co-first authors. The authors declare that they have no competing interests.

References

1. Li Y, Huang J, Lu J, et al. The role and mechanism of Asian medicinal plants in treating skin pigmentary disorders. *J Ethnopharmacol*. 2019;245:112173. doi:10.1016/j.jep.2019.112173
2. Choi W, Miyamura Y, Wolber R, et al. Regulation of human skin pigmentation in situ by repetitive UV exposure: molecular characterization of responses to UVA and/or UVB. *J Invest Dermatol*. 2010;130(6):1685–1696. doi:10.1038/jid.2010.5
3. Wu YY, Tian S, Miao MS. Analysis of the use of animal models of chloasma based on data mining. *Chin J Comparat Med*. 2020;30(8):70–75.
4. You YJ, Wu PY, Liu YJ, et al. Sesamol Inhibited Ultraviolet Radiation-Induced Hyperpigmentation and Damage in C57BL/6 Mouse Skin. *Antioxidants*. 2019;8(7):207. doi:10.3390/antiox8070207
5. Naganumaa M, Yagi E, Fukuda M. Delayed induction of pigmented spots on UVB-irradiated hairless mice. *J Dermatol Sci*. 2001;25(1):29–35. doi:10.1016/S0923-1811(00)00098-0
6. Liu XY, Fan QY, Gao J. Preparation and reflection on animal models of melasma. *Chin J Comparat Med*. 2021;31(10):54–60.
7. Todo H. Transdermal permeation of drugs in various animal species. *Pharmaceutics*. 2017;9(3):33. doi:10.3390/pharmaceutics9030033
8. Briggaman RA. Epidermal-dermal interactions in adult skin. *J Invest Dermatol*. 1982;79(Suppl 1):21s–24s. doi:10.1111/1523-1747.ep12544628
9. Hong SD, Yoon DY, Lee S, Han SB, Kim Y. Antimelanogenic chemicals with in vivo efficacy against skin pigmentation in Guinea pigs. *Arch Pharm Res*. 2014;37(10):1241–1251. doi:10.1007/s12272-014-0447-9
10. Schäfer M, Schneider M, Müller T, et al. Spatial tissue proteomics reveals distinct landscapes of heterogeneity in cutaneous papillomavirus-induced keratinocyte carcinomas. *J Med Virol*. 2023;95(6):e28850. doi:10.1002/jmv.28850
11. Hedrich V, Breitenecker K, Ortmayr G, et al. PRAME is a novel target of tumor-intrinsic Gas6/Axl activation and promotes cancer cell invasion in hepatocellular carcinoma. *Cancers*. 2023;15(9):2415. doi:10.3390/cancers15092415
12. Szklarczyk D, Kirsch R, Koutrouli M, et al. The STRING database in 2023: protein-protein association networks and functional enrichment analyses for any sequenced genome of interest. *Nucleic Acids Res*. 2023;51(D1):D638–D646. doi:10.1093/nar/gkac1000
13. Shannon P, Markiel A, Ozier O, et al. Cytoscape: a software environment for integrated models of biomolecular interaction networks. *Genome Res*. 2003;13(11):2498–2504. doi:10.1101/gr.1239303
14. D'Orazio J, Jarrett S, Amaro-Ortiz A, Scott T. UV radiation and the skin. *Int J Mol Sci*. 2013;14(6):12222–12248. doi:10.3390/ijms140612222
15. Cho YH, Park JE, Lim DS, Lee JS. Tranexamic acid inhibits melanogenesis by activating the autophagy system in cultured melanoma cells. *J Dermatol Sci*. 2017;88(1):96–102. doi:10.1016/j.jdermsci.2017.05.019
16. Tobiishi M, Haratake A, Kaminaga H, et al. Pigmentation in intrinsically aged skin of A1 Guinea pigs. *Pigment Cell Res*. 2004;17(6):651–658. doi:10.1111/j.1600-0749.2004.00183.x
17. Im S, Lee ES, Kim W, et al. Donor specific response of estrogen and progesterone on cultured human melanocytes. *J Korean Med Sci*. 2002;17(1):58–64. doi:10.3346/jkms.2002.17.1.58
18. Tamega Ade A, Miot HA, Moco NP, Silva MG, Marques ME, Miot LD. Gene and protein expression of oestrogen-beta and progesterone receptors in facial melasma and adjacent healthy skin in women. *Int J Cosmet Sci*. 2015;37(2):222–228. doi:10.1111/ics.12186
19. Handa S, De D, Khullar G, Radotra BD, Sachdeva N. The clinicoaetiological, hormonal and histopathological characteristics of melasma in men. *Clin Exp Dermatol*. 2018;43(1):36–41. doi:10.1111/ced.13234
20. Taraborrelli S. Physiology, production and action of progesterone. *Acta Obstet Gynecol Scand*. 2015;94(Suppl 161):8–16. doi:10.1111/aogs.12771
21. Del Bino S, Sok J, Bessac E, Bernerd F. Relationship between skin response to ultraviolet exposure and skin color type. *Pigment Cell Res*. 2006;19(6):606–614. doi:10.1111/j.1600-0749.2006.00338.x
22. Liu X, Wang T, Su Z. Research status on animal models for melasma. *Chin J Exper Traditional Med Form*. 2020;26(23):200–208.
23. Del Bino S, Duval C, Bernerd F. Clinical and biological characterization of skin pigmentation diversity and its consequences on UV impact. *Int J Mol Sci*. 2018;19(9):2668. doi:10.3390/ijms19092668
24. Yardman-Frank JM, Fisher DE. Skin pigmentation and its control: from ultraviolet radiation to stem cells. *Exp Dermatol*. 2021;30(4):560–571. doi:10.1111/exd.14260
25. Videira IF, Moura DF, Magina S. Mechanisms regulating melanogenesis. *An Bras Dermatol*. 2013;88(1):76–83. doi:10.1590/S0365-05962013000100009
26. Bellei B, Picardo M. Premature cell senescence in human skin: dual face in chronic acquired pigmentary disorders. *Ageing Res Rev*. 2020;57:100981. doi:10.1016/j.arr.2019.100981
27. Filoni A, Mariano M, Cameli N. Melasma: how hormones can modulate skin pigmentation. *J Cosmet Dermatol*. 2019;18(2):458–463. doi:10.1111/jocd.12877
28. Gautam M, Patil S, Nadkarni N, Sandhu M, Godse K, Setia M. Histopathological comparison of lesional and perilesional skin in melasma: a cross-sectional analysis. *Indian J Dermatol Venereol Leprol*. 2019;85(4):367–373. doi:10.4103/ijdvl.IJDVL_866_17